Exposure of real estate properties to the 2018 Hurricane Florence flooding

Marco Tedesco[1], Steven McAlpine[2] and Jeremy R. Porter[3, 4]

1) Lamont-Doherty Earth Observatory of the Columbia University
2) FirstStreet Foundation
3) City University of New York - Quantitative Methods in the Social Sciences
4) Columbia University Medical Center - Environmental Health Sciences

Correspondence to: M.Tedesco (mtedesco@ldeo.columbia.edu)

Abstract. Quantifying the potential exposure of property to damages associated with storm surges, extreme weather, and hurricanes is fundamental to developing frameworks that can be used to conceive and implement mitigation plans as well as support urban development that accounts for such events. In this study, we aim at quantifying the total value and area of properties exposed to the flooding associated with Hurricane Florence that occurred in September 2018. To this aim, we implement an approach for the identification of affected areas by generating a map of the maximum flood extent obtained from a combination of the flood extent produced by the Federal Emergency Management Agency's (FEMA) water marks with those obtained from spaceborne radar remote sensing data. The use of radar in the creation of the flood extent allows for those properties commonly missed by FEMA's interpolation methods, especially from pluvial/non-fluvial sources, and can be used in more accurately estimating the exposure and market-value of properties to event-specific flooding. Lastly, we study and quantify how the urban development over the past decades in the regions flooded by Hurricane Florence might have impacted the exposure of properties to present-day storms and floods. This approach is conceptually similar to what experts are addressing as the "expanding bull's-eye effect" in which ''targets" of geophysical hazards, such as people and their built environments, are enlarging as populations grow and spread. Our results indicate that the total value of property exposed to flood during Hurricane Florence was $52B (in 2018 USD), with this value increasing from ~ $10B at the beginning of the past century to the final amount based on the expansion of number of properties

exposed. We also found that, despite the decrease in the number of properties built during the decade before Florence, much of the new construction was in proximity to permanent water bodies, hence increasing exposure to flooding. Ultimately, the results of this paper provide a new tool for shedding light on the relationships between urban development in coastal areas and the flooding of those areas, which is estimated to increase in view of projected increasing sea level rise, storm surges and strength of storms.

1 Introduction and rationale

The projected rise in sea level, increased floods and storm surge and associated consequences over the 21st century has the potential to do immense economic harm. The economic impact is particularly worrisome in the U.S. because the most valuable real estate, densest communities, and most productive economic engines are situated disproportionately in coastal regions (Fu et. al., 2016; NOAA, 2013; Kildow et. al., 2014). Recent research has highlighted an ongoing economic signal associated with high-probability flooding events and real estate transactions in coastal communities that can be observed with historical data (see McAlpine and Porter, 2018; Keenan et. al. 2018; and Bernstein et. al. 2019), suggesting that sea level rise (SLR) is already producing negative economic consequences on coastal communities. Furthermore, there is abundant evidence indicating that we are only seeing the first signs of a much more problematic issue both in terms of the flooding scale and the magnitude of associated economic losses (see Fu et al, 2016; Hallegatte et al., 2011; Bin et al., 2011; Bin et al. 2008; Parsons and Powell 2008; Michael 2007). In this regard, a SLR of ~ 2 meters (e.g., six feet) would flood roughly 100,000 homes only in New York City, with a total value of $39 billion (note that we use 2018 as a reference for the dollar year throughout this manuscript unless otherwise mentioned); a 3 meters (ten-foot) rise would flood 300,000 homes and property with a value of almost $100 billion (Union of Concerned Scientists, UCSUSA, Accessed 29 June, 2019). The equivalent figures for Miami are 54,000 homes and property valued at $14 billion at risk with a ~ 2 meters rise and 130,000 homes and property valued at $32 billion for a ~ 3 meters rise.

Recent events such as hurricanes Katrina, Irma and Florence have been highlighting even more the issues related to floods and extreme events. In particular, Florence was one of the most devastating hurricanes in history as it combined storm surge, strong winds and extreme precipitation. It began as a tropical storm on 1 September, 2018 over the Cabo Verde Islands off the coast of West Africa and peaked as a Category 4 hurricane with winds up to 225 Km/hour before making landfall as a Category 1 hurricane on 14 September, 2018 over Wrightsville Beach, North Carolina. By 5 p.m. on Friday, 14 September, 2018 Florence was downgraded to a tropical storm and early on Sunday, 16 September it became a tropical depression, with winds of about 360 Km/hour. At least 51 people died as a consequence of flooding associated with rain records (up to 3 feet of rain in some areas according to the Weather Service), with more than 400,000 houses without power and a total damage of $24 billion (https://www.ncdc.noaa.gov/billions/events.pdf).

The human cost of Hurricane Florence was a reminder of the power of such storms and these storms are likely becoming more impactful as their surge reaches further inland due to changing tracks, increased strength, and rising seas. The increasing exposure of the public and properties to events similar to Hurricane Florence has unintended consequences of raising the awareness and concern to all types of climate related events (Borenstien and Fingerhut, 2019). Such is likely the case in much of the recent research on real-estate market responses to higher-probability flooding associated with nuisance tidal flooding events (McAlpine and Porter, 2018). In their study, MacAlpine and Porter (2018) found that properties in Miami-Dade County at risk of frequent tidal flooding had lost over $430 million in property value relative to homes that were not a risk of repeated tidal flooding events. Likewise, and also centered in the Miami-Dade region, Keenan et al. (2018) found that homes at lower elevations were being penalized on the market relative to homes at higher elevations. Moreover, in another analysis, Bernstein et al. (2018) found a similar penalty for homes at risk of flooding from increase in SLR, but found that this penalty was primarily driven by investors and an uneven access to information associated with risk. All of these studies identify an increase in awareness of SLR related flooding events and all document the fact that this trend is relatively new (since about the middle of the last decade). Of particular importance to the recent market response is the fact that increased probability is an important driving force. In the work undertaken by Bernstein et al. (2019), for example, the price

penalty for homes at risk of flooding is explicitly driven by the sophistication of investors and their access to risk tools aimed at helping them to make decisions about property value, and long-term appreciation over time. McAlpine and Porter (2018) also found, in this regard, that risk associated with being impacted by a Category 1 hurricane is correlated with potential loss property value, but not the probability of being impacted by a higher Category storm. In each of these cases, the research suggests that the real-estate market is becoming more sensitive to the probability of damage associated with inundation from flooding events due to rising seas, storm surges, nuisance flooding and consequences of a changing climate. On the other hand, research out of University of Pennsylvania's Wharton Risk Center by Kunreuther et al. (2019) found that the elasticity concerning the housing market tends to show quick recoveries in areas where the experience of climate catastrophes is characterized as a market shock. Market shocks are generally thought of a one-time (or contiguous time period) events that negatively impact the housing market. Due to the nature of market shocks being lower probability and harder to predict, the housing market tends to see them as unlikely and related to collective internalizations associated with myopia, amnesia, optimism, inertia, simplification, and herding (Kunreuther et.al., 2019). However, market stressors are ubiquitous, high-probability, events that are generally predictable and have historical certainty. In the context in which we are working, increased and unmanageable tidal flooding could be considered a market stressor, while the impact of a single hurricane event could constitute a market shock. Historically, market shocks (such as hurricanes) are much more expensive, in terms of actual economic impacts, and consume more media attention, in terms of the coverage of the events.

Several studies have recently focused on assessing damages from hurricane Florence. Roberson et al. (2019) use overhead imagery, including synthetic aperture radar (SAR) and optical data, to study the impact of Florence on livestock wastewaters and crop health. Srikanto et al. (2019) study the spatial distribution of fatalities and associated demographics, indicating that 93 % of the affected buildings were residential structures. The proper quantification of the impact of Hurricane Florence (or more in general of extreme events) is not only helpful for addressing the recovery of the communities impacted by the event but also to provide tools to policy makers, urban planners and city managers that will ultimately guide them through the decision process of reducing the impacts of future events. If it is true,

indeed, that climate change is and will be influencing the frequency and strength of storms and floods, it is also true that the exposure of anthropogenic structures and lives is a function of urbanization factors such as, for example, the building of new properties in proximity of the coast and of body waters. In this context, it becomes crucial to understand and quantify how urban development has impacted the exposure of properties and population to present-day storms and floods. For example, one of the most devastating hurricanes over the same region before Florence was Hurricane Hugo, reaching the Carolinas on 10 September 1989, with winds up to 260 Km/hour and a total estimated damage of $9.45 billion (in 1989 USD, equivalent to ~ $19B of 2018 USD) and 60 fatalities. Unlike 1989, we have today improved observational and modeling tools that allow us to better estimate the maximum flood extent, a key parameter needed to estimate the potential exposure to damage of properties and other infrastructures. From a modeling point of view, hydrological and hydrodynamic models, in conjunction with improved digital elevation models and the ingestion of gage observation or observation of high water marks, offer the opportunity to generate estimates of maximum flood extent (FEMA, 2019).

We aim at understanding the usefulness of remotely sensed satellite data as a method for the identification of impacted areas and for delineating the maximum flood extent. Specifically, we report results concerning the mapping of the flood extent associated with Hurricane Florence estimated from SAR data and compare such extent with the maximum flood extent provided by FEMA. From that exposure, we are able to quantify the property value and total area exposed to Hurricane Florence by combining the flood extent coverage with a database containing publicly available property value attributes. Despite recent studies have started to focus on the spatio-temporal variability of property values and human settlements in hurricane-prone areas (e.g., Huang et al., 2019) and on the market responses to increases in observed flooding events (e.g., McAlpine and Porter, 2019; Keenan et. al, 2018), no study, to our knowledge, has focused on the impact of urban growth on the property exposed to Hurricane Florence. Addressing this point is crucial to account for those impacts related to the choices that our society makes to continue the expansion of urban areas and that have been addressed by experts as the “bull’s-eye expanding effect” (Ashley and Strader, 2018), in which ‘‘targets” of geophysical hazards, such as people and their built environments, are enlarging as populations grow and spread. The term “bull’s-eye” is here used to define the eye or center of a storm. Our approach is

complementary to those approaches focusing on the bull's eye effect and to those calculating the impact of floods under future climate scenarios (e.g., sea level rise or storm surge is changing but the properties distribution remains the same). Specifically, we assess the potential exposure of properties using a dataset containing, among other things, when each property was built and use that information to estimate the potential exposure of buildings to Hurricane Florence should have occurred in the past decades.

2 Data and Methods

2.1 Sentinel-1 radar data and identification of inundated areas

From an observational point of view, spaceborne and airborne remote sensing (e.g., Schumann et al., 2011), as well as UAV-based approaches (e.g., Gebrehiwot et al., 2019) offer powerful tools to monitor flood extent (e.g., Domeneghetti et al., 2019; Kordelas et al., 2018; Shumann et al., 2018a, 2018b, Giordan et al., 2018). Optical data can map the presence of surface water at relatively high spatial resolution and accuracy (e.g., Kordelas et al., 2018) but it is limited by the presence of clouds (Shumann et al., 2018). On the other hand, datasets collected in the microwave region, such as those collected by Synthetic Aperture Radar (SAR), are not limited by the presence of clouds (Shumann et al., 2018, Manavalan, 2017; Huang et al., 2018). The recent launch of Sentinel-1 ESA sensors in September 2014 (Sentinel-1A) and April 2016 (Sentinel-1B, https://sentinel.esa.int/web/sentinel/missions/sentinel-1) allows mapping of flood extent at unprecedented temporal and spatial resolutions. The combination of the two sensors provides a nominal 6-day repeat cycle over the equator and 12-day repeat cycle over North America (Torres et al., 2012) at a horizontal spatial resolution of the SAR data is 10 m. For the purpose of this study, we obtained Sentinel-1 data from the National Aeronautics and Space Administration Alaska Satellite Facility (NASA/ASF, https://earthdata.nasa.gov/about/daacs/daac-asf). More information on the Sentinel-1 sensors can be found at https://sentinel.esa.int/web/sentinel/missions/sentinel-1. Specific details on the SAR-based approach used in this study are reported in the supplementary material.

2.2 FEMA Maximum water extent during Florence

We supplement the radar-derived flood extent with the FEMA's High Water Mark-based Depth Grids and Inundation Polygons from observed and collected Hurricane Florence data. High Water Marks (HWM) are point data collected using high resolution Real Time Kinematic (RTK) GPS systems or other methods. HWM points represent the highest extent of riverine flood or coastal storm surge inundation. The raw data is available at the FEMA Natural Hazard Risk Assessment Program (NHRAP) site and were downloaded for all basins available per FEMAs collection efforts following the hurricane event (https://data.femadata.com/FIMA/NHRAP/Florence/).

The FEMA Maximum Water Extent is distributed as a GIS raster file created to represent the extent of riverine or coastal storm inundation following larger flooding events. The file is created as a derived product following the creation of the Maximum Depth Grids raster file, which is obtained using FEMA HWM data and FEMA's Digital Flood Insurance Rate Map (DRIRM) Base Flood Elevations (LIDAR based elevation data). Using those datasets, a grid is obtained to estimate the height of water at any given point between HWM based on base elevation. From this, we extracted a secondary file measuring only the extent of inundation from the storm surge. The FEMA dataset is distributed as an ARCGIS® geodatabase (.gdb format) and we rasterized it at a spatial resolution of 10 m to match the spatial resolution of the SAR data. More information on the FEMA approach for estimating maximum flood extent can be found at https://data.femadata.com/FIMA/NHRAP/Florence.

2.3 Property database

Property value data is compiled from each individual property's county assessor in the form of the property tax assessed value. The data were obtained from a third party provider, ATTOM™ Data Solutions, which provides high quality parcel level information on all properties in the United States and in a value added format (https://www.attomdata.com). The process by which the data are compiled relies solely on publicly available data and the processing, cleansing, standardizing of that data in order to make it available in a user-friendly format. The data used in this analysis include the property's last recorded assessment value for all properties within the states of North and South Carolina as well as the year when the property was built. Each county's assessment process varies and, as such, the data are

subject to known potential limitations associated with the timing and frequency of home assessments undertaken by local county officials in which the property is located. However, the data also give us the best available comprehensive look at tax base value in a geo-located format for comparison to our storm surge coverage file.

3 Results and discussion

3.1 Assessment of remote-sensing derived areas vs. FEMA maximum water extent

Inundated areas (including permanent water bodies) obtained from Sentinel-1 data and FEMA are reported, respectively, as blue (radar) and red (FEMA) regions in Figure 1a. We used a total of 12 Sentinel-1 images collected between 14 September and 19 September, 2018 and whose footprints are shown in the inset in the top left corner of Figure 1b. Specific names and acquisition times of the radar images are reported in the Supplementary material. We used the 12 images in order to maximize the covered area and to account for the temporal evolution of surface water after the landfall of Hurricane Florence associated with heavy, persistent rainfall.

The comparison between the maximum water extent estimated by FEMA and the water extent mask obtained from Sentinel-1 indicates a matching score (defined here as the percentage of flooded pixels identified by Sentinel-1 with respect to the total number of flooded pixels identified by FEMA) of 11.3 % and a commission error (defined as the relative percentage number of pixels when Sentinel-1 detects flooded areas but FEMA does not with respect to the total number of FEMA flooded pixels) of 9.2 %. We remind here that the FEMA map is based on a combination of modeled and measured quantities and might miss flooding associated with heavy rains, as in the case of Hurricane Florence. Consequently, it is possible that some areas that were flooded according to the radar images were not included in the FEMA maps. As an example, Figure 2 shows the maximum water extent from FEMA (red) together with the one derived from Sentinel-1 data (blue) nearby the town of Bennettsville, SC (34.6174° N, 79.6848° W). Green dots show the location of the properties within our database. We note that the radar sensor is detecting water over agricultural fields that are not marked by the FEMA maps as flooded, showing a potential improvement over the FEMA maps. Our analysis of the Sentinel-1

backscattering coefficients (not shown here) indicates that the backscattering values recorded for those regions where flood was identified by the radar were relatively low (e.g., well below the threshold value and on the order of ~ -20 dB or below), indicating that those were, indeed, inundated areas.

Another factor complicating the comparison between Sentinel-1 and FEMA inundated regions regards the acquisition time of the radar images, which are collected before or after the time of the maximum water extent. Figure 3a shows the time series of the water height (mean sea level in meters) for the ocean tide gauge located in Wrightsville Beach, NC (id #8658163), where Hurricane Florence made landfall. Maximum water height was reached on the same day around 15:00 UTC. The image also shows the acquisition time of the Sentinel-1B (14 September, 2018, 11:15:05, UTC) and Sentinel-1A (14 September, 2018, 23:05:48, UTC) as vertical, dashed lines, indicating that such images were, indeed, acquired before and after the time when the water reached the maximum extent. River gages data also show that, because of the heavy precipitation, the maximum water discharge and gage heights inland occurred a few days after hurricane Florence made landfall. In this regard, Figures 3b and 3c show, respectively, the daily discharge (in cubic meters per hour) and daily gage height (in meters) recorded at the river gauge station of Lumberton, NC (34.6182° N, 79.0086° W), located about 150 km inland. The data shows the peak discharge and water heights late in the evening of 17 September, 2018. For this same area the radar data were collected when the tide gage recorded peak values, confirming the usefulness of this tool to capture flooding that might not have been captured by FEMA. As a further example, we show in Figure 4 the flooded areas detected by Sentinel-1 (blue filled regions) on 19 September, 2018 nearby Pasley, Duplin County, NC (34.7854° N, 77.9005° W) and a photograph of the same area collected on 18 September, 2018 by the NOAA Remote Sensing Division to support emergency response requirements (https://storms.ngs.noaa.gov/storms/florence/index.html#7/35.360/-77.820). The figure shows that most of the flooded areas identified within the NOAA photograph are properly captured by Sentinel-1, with differences between the two also due to the different acquisition times. For this area, the FEMA map does not indicate any flooding, confirming the complementary nature of the radar dataset.

Given these considerations, for this study we merge the FEMA and Sentinel-1 flood extent maps to generate a maximum composite flood extent map that will be used to assess the property exposure to

Hurricane Florence flooding. We will refer to this dataset simply as the "maximum flood extent" in the remaining sections of the manuscript.

3.2 Exposure of property to Hurricane Florence flooding

Figure 5 shows the spatial distribution of the properties within our database overlaid with an image of the eye of Hurricane Florence when it made landfall. Our analysis indicates that the total area of properties affected by the maximum flood extent water was 70,964,700 m^2 (e.g., physical footprint) being 17.55 % of the total area within our database. When considering only the flood extent estimated by Sentinel-1, the total area of properties affected by the flood reduces to 3.2 %, corresponding to 12,939,432 m^2. In order, to quantify potential biases associated with co-registration issues or resampling procedures, we also computed the number of properties exposed to the extent of our permanent body water dataset. Our analysis shows that less than 0.2 % of properties was overlapping with the permanent body waters. Consequently, we removed these properties from our analysis.

The total property value exposed estimated using the maximum flood extent is $52,079,520,584 (2018 USD, corresponding to ~ 9.5 % of the total property value within our database). The exposed property value is $9,437,931,512 when considering only Sentinel-1 data. The exposed property value computed over the flooded regions estimated by Sentinel-1 but not by FEMA is $3,278,098,601. The relatively small exposure area and property values obtained with Sentinel-1 are due to the limitations discussed above and the difficulties of SAR data to detect flooding in urban areas (e.g., Notti et al., 2018), where the basic assumption on the physical processes leading to the detection of flooded areas by Sentinel-1 is violated by the presence of dense vegetation or buildings. In this case, indeed, the radar signal will bounce on the vertical structures (e.g., buildings and trees) after being reflected by the water surface, increasing the amount of energy reaching the radar receivers rather than reducing it, as expected in the absence of vegetation or urban structures (e.g., Schumann, 2018a, 2018b). Another reason for the underestimation of property exposure derived from Sentinel-1 data can be seen in Figure 4. Here it is evident that Sentinel-1 is detecting flooding over rural and agricultural areas, where the number of properties is smaller than in highly density populated areas.

In Figure 6 we report the distribution of the number of properties exposed to flooding as a function of the corresponding property value. A power law function (as reported in Eq. 1)

$$Y = a*x^n \quad \text{(Eq. 1)}$$

fitting the histogram is also plotted as a dashed, black line with *a* and *n* obtained from the fitting as $a = 1.9544*10^6$ and n = -1.1216. The power law function here selected was chosen after testing several functions (e.g., exponential decay, logarithmic, etc.) as the one showing the highest regression coefficient ($R = 0.99$). According to Zillow©, the median home values in North Carolina and South Carolina are, respectively, $ 184,200 (North Carolina) and $ 166,300 (South Carolina) with a median price of homes of $196,600 in the case of North Carolina and $187,800 for South Carolina. We use these estimates to set to $200k the median price within our database and evaluate the number of properties this value using Eq. 1. We find that 40 % of the properties exposed to Hurricane Florence flooding were below the threshold value. The properties valued between $200k and $500k account for another 25 % whereas the properties with values between $500k and $1M account for another 25 %. As a reference, the total number of properties valued below $200k represent ~ 50 % of our database, those between $200k and $500k are ~ 25 % and those between $500k and $1M roughly 15 %.

Distance from water bodies, especially coastal and riverine bodies, is also a useful indicator of properties vulnerability and potential exposure in hurricane prone areas. Consequently, we expanded our analysis to consider the distance of the properties that were flooded during Florence within our database from permanent water bodies (Figure 7). Values along the x-axis in the plot are obtained as the minimum distance from any of the closest element of the permanent water bodies mask (e.g. ocean, rivers, lakes) to each property within our database. The figure also shows the exponential decay function fitting the histogram and the corresponding fitting parameters. From this analysis, we estimate that ~ 95 % of the number of properties exposed to flooding fell within 10 km from body waters. This number increases when considering only the distance from the ocean because of the inland flooding associated with heavy precipitation. We, therefore, use the distance of 10 km as a maximum distance for

studying the relationship between new properties, their distance from water bodies and the exposure to the Florence flood extent.

3.3 Impact of expansion of urban areas on property exposure

Addressing this point is crucial to account for those impacts related to urban growth and the expansion of urban areas as addressed by experts when considering the so-called the "bull's-eye expanding effect" (Ashley and Strader, 2018), in which ''targets" of geophysical hazards, such as people and their built environments, are enlarging as populations grow and spread. In this case, the bull's eye expansion does not refer to the increased storm size but rather to the area where the impact of the geophysical hazard is occurring, expanding because of the urbanization process over the past decades. This concept is well synthesized in what has been named "the expanding bull's-eye effect" (Ashley and Strader, 2016), arguing that ''targets''—people and their built environments— of geophysical hazards are enlarging as populations grow and spread. We point out that, to demonstrate their bull's-eye effect, Ashley & Strader (2016) work with a semi-empirical spatio-temporal model of housing stock in tornado zones over time. A major difference between this study and Ashley and Strader (2016) is that in our case we have a snapshot of stock rather than a continuous record through time (i.e., annual records of all properties). This means that our dataset might be skewed toward newer properties as old buildings get replaced and that, despite the bull's eye expansion effect is evident from space, our properties dataset might only capture it indirectly. With this in mind, we calculated what would have been the property area and values exposed to the Florence flood should that have occurred 10, 50 or 100 years ago by using the information contained within our database on the years when properties were built. For the purpose of this analysis, we clarify that we are assuming the same sea levels and topography of today.

Figure 8 shows the spatial distribution of the properties within our database that were built during the a) 1800 – 1900, b) 1900 – 1950, c) 1950 – 2000 and d) 2000 – 2018 periods. We considered the first period as a 100-year one (Figure 8a) because of the relatively small number of properties that were built then. Most of the urban growth between 1900 and 1950 (Figure 9b) occurred inland and along the coast north of Wilmington, with a relatively small number of new properties built close to

water bodies (either rivers or ocean). An explosion in new properties occurred between 1950 and 2000 (Figure 8c), likely as a consequence of the economic stimulus following World War II. The period 2000 – 2018 shows a relatively smaller number of new properties with respect to the previous periods (Figure 8d). In this regard, our analysis performed on the 10-year period of number of properties built within our database (Figure 9) shows that before 2010 the number of houses built had been increasing exponentially ($Y = 5e\text{-}22 * \exp^{0.0314*X}$, $R = 0.99$, with X being the year) and that the number of new properties after 2010 drastically dropped, reaching values similar to those observed before the 1950s. This might be due to the 2008 "house crisis" that occurred during that period.

Figure 10 shows the time series of total value of exposed property (in 2018 $B). The inset reports the relative change of the exposed area and value between two consecutive time steps (10 years). Consistent with the results discussed above, a relatively small increase in the exposed property value occurs before the 1940s (from ~ $10B to ~ $12B). Urban expansion increases considerably after 1940s (Figure 8), reaching a maximum value of exposed property of ~ $52B in 2018. We fitted the increase in exposed property value after 1900 with an exponential function ($Y = a*\exp^{bX}$) and computed the coefficients providing best fitting ($a = 1.0627*1e^{-13}$, $b = 0.167$, $R = 0.97$). The maximum relative increase is reached around the year 2000 with an increase in properties exposed value of ~ $8B between two successive decades. After then, the relative change in exposed property values decreases to those obtained in the early 1950s.

As mentioned, distance from permanent water bodies can play a critical role in terms of exposure, with flooding due to Hurricane Florence reaching properties that were up to ~ 10 km from the closest water body. Therefore, we further studied how the property value evolved in terms of the distance from water bodies between 1800 and 2018. As an example, in Figure 11 we show the distribution of properties built during different periods in proximity of Wrightsville beach, where hurricane Florence made landfall. The figure clearly highlighs the expansion of urban areas along the coasts and water bodies, especially between 2000 and 2018. In Figure 12 we also show the total value of exposed properties within our database as a function of distance from water bodies between 1800 and 2000 (using a 25-year time step) and for the period 2000 – 2018. We note that the curves referring to early decades reach a plateau within a relatively short distance than those referring to later periods, with

the saturation values (e.g., the value when the curve becomes flat) being of the order of 1500m in the case of the 1975 – 2000 period. Differently from other periods, the one spanning between 2000 and 2018 does not show a saturation value with the distance from water bodies, with the exposed property values continuing to increase as the distance from water increases. This is an important aspect as it suggests that, despite the most recent decades were characterized by a relatively smaller number of new properties (Figure 9), the potential exposure to Florence of such properties was higher because of the higher number of the exposed properties close to body waters.

4 Conclusions

Increased flooding associated with sea level rise, storm surges and other extreme events has the potential to economically disrupt many areas around the world, with most of valuable real-estate, densest communities and most productive economic engines situated in coastal regions. The specific goal of our study was to quantify the exposure of properties to the flooding associated with Hurricane Florence that hit the Carolinas in September 2018 and to study how the spatio-temporal evolution of new built properties along the most recent decades has impacted the property exposure. It is important to note that much of the vulnerability associated with building development in these areas should be considered independent of climate change to this point. However, moving forward, these types of storms are expected to increase in intensity and the link between climate change and potential exposure is likely to be tied more closely together. In fact, we are already seeing these trends as they relate to tidal flooding events and one might expect that the low probability-larger storms are likely to become more linked to our changing climate as well.

In order, to properly quantify the exposure of properties to Florence flooding, we developed a maximum flood extent map from the combination of the FEMA maximum extent map (generated through the merging of high water marks) and the flooded areas detected by means of spaceborne radar data acquired by the ESA Sentinel-1 sensors. We found that the total value of property exposed to flooding was ~ $52B and that this value has increased exponentially from ~ $10B (2018 $US) in the early 1900s. This is due to the increase in the number of properties that came to a halt at the beginning

of the 2000s, likely as a consequence of the 2008 housing crisis, when the number of new properties built after 2010 was almost half of those built only a decade before. Despite this, the exposure to Florence flooding for those properties built after 2000 continued increasing, because of the number of new properties built within proximity of permanent water bodies and coastlines.

Our work cannot only provide new insights for policy makers and city planners but it also does provide a tool to better estimate how the property market will respond to future disasters. Recent work (e.g., McAlpine and Porter, 2018; Keenan et al., 2018) has found that homes at lower elevations were being penalized on the market relative to homes at higher elevations and that houses exposed to sea level rise sell for approximately 7% less than observably equivalent unexposed properties equidistant from the beach (Bernstein et al., 2019). For our future work, we plan to expand our analysis to other modern-day (e.g. Irma, Michael, Katrina and Sandy) and historical (e.g. Hugo in 1989) hurricanes to address similar questions to those addressed in this study. Moreover, we plan to improve the detection of maximum flood extent through the implementation of machine-learning techniques combining radar maps with tide gage interpolated data and other ancillary information. Lastly, the combination of the knowledge on how property distribution changed along the years in conjunction with outputs of physical or probabilistic models that can separate the different contributions associated to flood due to sea level rise, storm surge and rain will allow to properly quantify what is the impact of the different components of the climate-economic system on the total exposure and, eventually, damage. This will provide a crucial tool for policy makers, governments, citizens and those who are, rightly, interested in quantifying the impact of climate change on the economic and house markets.

Author's contribution.

MT conceived the study and wrote the first draft of the manuscript. JP and SM provided and analyzed the property data, permanent water bodies and LULC data. MT developed and implemented the code for the radar dataset. All authors contributed to the final analysis and final version of the manuscript.

Acknowledgments.

MT acknowledges financial support from Columbia University through the RISE program and from FirstStreet foundation.

Code availability. We used a combination of publicly available software and codes developed ad-hoc for the purposes of this study. Specifically, the ESA SNAP software used to pre-process the Sentinel datasets is available at http://step.esa.int/main/download/snap-download/. We also used QGIS 3.4 to export the property data into a shapefile and to analyze the permanent body waters and the FEMA maximum flood extent data. The software is available at https://qgis.org/en/site/forusers/download.html. We developed in-house codes in Matlab for mapping flooded areas from radar data and to perform the analysis of the exposed property values. These are available upon request to the corresponding author at mtedesco@ldeo.columbia.edu

Data availability. Sentinel1 data is freely available at https://earthdata.nasa.gov/about/daacs/daac-asf. The dataset containing the permanent water bodies is available at https://fwsprimary.wim.usgs.gov/wetlands/apps/wetlands-mapper/. Land use land cover attributes obtained from the National Geospatial Data Asset (NGDA) Land Use Land Cover (LULC) dataset is available at (https://www.sciencebase.gov/catalog/item/581d050ce4b08da350d52363. Maximum water extent by FEMA is available at https://data.femadata.com/FIMA/NHRAP/Florence/. Property value data is compiled from each individual property's county assessor in the form of the property tax assessed value and was obtained from ATTOM™ Data Solutions. Those interested in this dataset should reach out to the corresponding author mtedesco@ldeo.columbia.edu or can be obtained at www.attom.com.

Competing interest. The authors declare no competing interest.

References

Ashley, W. S., and Strader, S. M.: Recipe for disaster: How the dynamic ingredients of risk and exposure are changing the tornado disaster landscape. *Bulletin of the American Meteorological Society,* 97, 767-786, 2016.

Ashman, K.M., Bird, C.M., and Zepf, S.E.: Detecting bimodality in astronomical datasets, *Astronomical. Journal,* vol. 108, no. 6, pp. 2348–2361, 1994.

Bazi, Y., Bruzzone, L., and Melgani, F.: An unsupervised approach based on the generalized Gaussian model to automatic change detection in multitemporal SAR images,*IEEE Trans. Geosci. Remote Sens.*, vol. 43, no. 4, pp. 874–887, 2005.

Bernstein, A., Gustafson, M. and Lewis, R.: Disaster on the Horizon: The Price Effect of Sea Level Rise. *Journal of Financial Economics*. Forthcoming (as of 06/2019: available at: http://dx.doi.org/10.2139/ssrn.3073842, 2019.

Bin, O., Crawford, T., Kruse, J., & Landry, C.: Viewscapes and Flood Hazard: Coastal Housing Market Response to Amenities and Risk. *Land Economics*, 84(3), 434-448, 2008.

Bin, O., Poulter, B., Dumas, C.F., Whitehead, J.C.: Measuring the impact of sea level rise on coastal real estate: a hedonic property model approach. *J. Reg. Sci*. 51 (4), 751-767, 2011.

Borenstein, S., and H. Fingerhut: Most Americans see weather disasters worsening. AP-NORC Poll; Sept. 5th, 2019.

Chini, M., Hostache, R., Giustarini, L., and Matgen,P.: A hierarchical split-based approach for parametric thresholding of SAR images: Flood inundation as a test case, *IEEE Trans. Geosci. Remote Sens.*, vol. 55, no. 12, pp. 6975–6988, 2017.

Chini, M., Pelich, R., Pulvirenti, L., Pierdicca, N., Hostache, R., and Matgen, P.: Sentinel-1 InSAR Coherence to Detect Floodwater in Urban Areas: Houston and Hurricane Harvey as A Test Case, *Remote Sens*., 11, 107; doi:10.3390/rs11020107, 2019.

Domeneghetti, A., Schumann, Guy J.-P., and Tarpanelli, A.: Preface: Remote Sensing for Flood Mapping and Monitoring of Flood Dynamics, *Remote Sens*., 11, 943; doi:10.3390/rs11080943, 2019.

FEMA Standard Operating Procedure for Hazus Flood Level 2 Analysis. https://www.fema.gov/media-library-data/1530821743439-e16c13c1f6266bbe374dc00a00ac9910/Hazus_Flood_Model_SOP_level2analysis.pdf, Accessed June 6th, 2019.

Fu, X., Song, J., Sun, B., Peng,Z.: "Living on the edge": Estimating the economic cost of sea level rise on coastal real estate in the *Tampa Bay region, Florida, Ocean & Coastal Management*, Volume 133, December 2016, Pages 11-17, 2016.

Gebrehiwot, A., Hashemi-Beni, L., Thompson, G., Kordjamshidi, P. and Langan, T. E.: Deep Convolutional Neural Network for Flood Extent Mapping Using Unmanned Aerial Vehicles Data, *Sensors*, *19*(7), 1486; https://doi.org/10.3390/s19071486, 2019.

Giordan, D., Notti, D., Villa, A., Zucca, F., Calò, F., Pepe, A., Dutto, F., Pari, P., Baldo, M., and Allasia, P.: Low cost, multiscale and multi-sensor application for flooded area mapping, *Nat. Hazards Earth Syst. Sci.*, 18, 1493-1516, https://doi.org/10.5194/nhess-18-1493-2018, 2018.

Hallegatte, S., Ranger, N., Mestre, O., Dumas, P., Corfee-Morlot, J., Herweijer, C., Wood, R.M. Assessing climate change impacts, sea level rise and storm surge risk in port cities: a case study on Copenhagen. *Clim. change* 104 (1), 113-137, 2011.

Huang, W., DeVries, B., Huang, C., Lang, M.W., Jones, J.W., Creed, I.F., Carroll, M.L.: Automated Extraction of Surface Water Extent from Sentinel-1 Data, *Remote Sens.*, 10, 797; doi:10.3390/rs10050797, 2018.

Huang, X., Wang, C. and Lu, J.: Understanding Spatiotemporal Development of Human Settlement in 5 Hurricane-prone Areas on U.S. Atlantic and Gulf Coasts using Nighttime Remote Sensing, *Nat. Hazards Earth Syst. Sci. Discuss*., https://doi.org/10.5194/nhess-2019-64, 2019.

Jin, S., Yang, L., Danielson, P., Homer, C., Fry, J., and Xian, G.: A comprehensive change detection method for updating the National Land Cover Database to circa 2011. *Remote Sensing of Environmen*t, 132: 159 – 175, 2013.

Jonkman, S. N., Godfroy, M., Sebastian, A., and Kolen, B.: Brief communication: Loss of life due to Hurricane Harvey, *Nat. Hazards Earth Syst. Sci.,* 18, 1073-1078, https://doi.org/10.5194/nhess-18-1073-2018, 2018.

Keenan, J.M., Hill, T., & A. Gumber. Climate Gentrification: From Theory to Empiricism in Miami-Dade County, Florida. *Environmental Research Letters.* 2018.

Kildow, J.T., Colgan, C.S., Scorse, J.D., Johnston, P., Nichols, M., 2014. State of the US Ocean and Coastal Economies 2014.

Kittler, J., and Illingworth, J.: Minimum error thresholding, *Pattern Recognit.*, vol. 19, no. 1, pp. 41–47, 1986.

Kunthreuther, H., Wachter, S., Kousky, C. and M. Lacour-Little: Flood Risk and the U.S. Housing Market, Risk Management and Decision Process Center; Working Paper, October, 2018.

Landuyt, L. Van Wesemael, A., Schumann, G., Hostache, R., Verhoest, N.E.C, and Van Coillie, F.M.B: Flood Mapping Based on Synthetic Aperture Radar: An Assessment of Established Approaches, *IEEE Trans. On Geosc*. And Remo. Sens., 57, 2, 2019.

Lee, J.-S., Wen, J.-H., Ainsworth, T.L., Chen, K.-S., Chen, A.J.: Improved sigma filter for speckle filtering of SAR imagery. *IEEE Trans. Geosci. Remote Sens*., 47, 202–213, 2009.

Manavalan, R.: SAR image analysis techniques for flood area mapping—Literature survey. *Earth Sci. Inf.*, *10*, 1–14., 2017.

McAlpine, S.A., and Porter, J.R.: Estimating the Local Impacts of Sea-Level Rise on Current Real-Estate Loses: A Housing Market Case Study in Miami-Dade, Florida. *Population Research and Policy Review*. 36(6): 871-895. 2018.

Michael, J. A. 2007. "Episodic Flooding and the Cost of Sea-Level Rise," *Ecological Economics*, 63, 149–159, 2007.

Moser and S. B. Serpico, "Generalized minimum-error thresholding for unsupervised change detection from SAR amplitude imagery," *IEEE Trans. Geosci. Remote Sens.*, vol. 44, no. 10, pp. 2972–2982, Oct. 2006.

NOAA. National Coastal Population Report: Population Trends from 1970 to 2020, 2013.

Notti, D., Giordan, D., Caló, F., Pepe, A., Zucca F. and Galve, J.P.: Potential and Limitations of Open Satellite Data for Flood Mapping, *Remote Sens.*, 10, 1673; doi: 10.3390/rs10111673, 2018.

Otsu,N.: A Threshold Selection Method from Gray-Level Histograms," in *IEEE Transactions on Systems, Man, and Cybernetics*, vol. 9, no. 1, pp. 62-66, doi: 10.1109/TSMC.1979.4310076, 1979.

Parsons, G. R. and Powell, M.: "Measuring the Cost of Beach Retreat," *Coastal Management*, 29, 91–103, 2001.

Roberson, M. W., Bell, A. L., Roberson, L. E., Walker, T.A.: Geospatial analytics of Hurricane Florence flooding effects using overhead imagery, Proceedings Volume 10992, *Geospatial Informatics IX;* 1099208, https://doi.org/10.1117/12.2519242, 2019.

Schumann, G. J-P., Brakenridge, G.R., Kettner, A.J., Kashif, R., and Niebuhr, E.: Assisting Flood Disaster Response with Earth Observation Data and Products: A Critical Assessment, *Remote Sens.*, 10, 1230; doi: 10.3390/rs10081230, 2018a.

Schumann, G.: Remote Sensing of Floods. *Oxford Research Encyclopedia of Natural Hazard Science.* 10.1093/acrefore/9780199389407.013.265, 2018b.

Schumann, G. J.-P., Neal, J. C., Mason, D. C., & Bates, P. D.: The accuracy of sequential aerial photography and SAR data for observing urban flood dynamics: A case study of the UK summer 2007 floods. *Remote Sensing of Environment*, 115, 2536–2546, 2011.

Srikanto, P., Ghebreyesus, D., and Hatim, O. S.: Brief Communication: Analysis of the Fatalities and Socio-Economic Impacts Caused by Hurricane Florence, *Geosciences*, *9*(2), 58; https://doi.org/10.3390/geosciences9020058, 2019.

Stone, M. H., and Cohen, S.: The influence of an extended Atlantic hurricane season on inland flooding potential in the southeastern United States, *Nat. Hazards Earth Syst. Sci.,* 17, 439-447, https://doi.org/10.5194/nhess-17-439-2017, 2017.

Torres, R., Snoeij, P., Geudtner, D., Bibby, D., Davidson, M., Attema, E., Potin, P., Rommen, B., Floury, N., Brown, M., Navas Traver, I., Deghaye, P., Duesmann, B., Rosich, B., Miranda, N., Bruno, C., L'Abbate, M., Croci, R., Pietropaolo, A., Huchler, M., Rostan, F.: GMES Sentinel-1 mission, *Remote Sensing of Environment*, Volume 120,2012,Pages 9-24,ISSN 0034-4257,https://doi.org/10.1016/j.rse.2011.05.028, 2012.

Twele, A., Cao, W., Plank, S., and Martinis,S.: Sentinel-1-based flood mapping: A fully automated processing chain, *Int. J. Remote Sens.*, vol. 37, no. 13, pp. 2990–3004, 2016.

Union of Concerned Scientists, UCSUSA, Underwater: Rising Seas, Chronic Floods, and the Implications for US Coastal Real Estate, Available at https://www.ucsusa.org/sites/default/files/attach/2018/06/underwater-analysis-full-report.pdf, Accessed 19 June, 2019.

Xian, G., Homer, C., Dewitz, J., Fry, J., Hossain, N., and Wickham, J.: The change of impervious surface area between 2001 and 2006 in the conterminous United States. *Photogrammetric Engineering and Remote Sensing*, Vol. 77(8): 758-762, 2011.

5 Figures

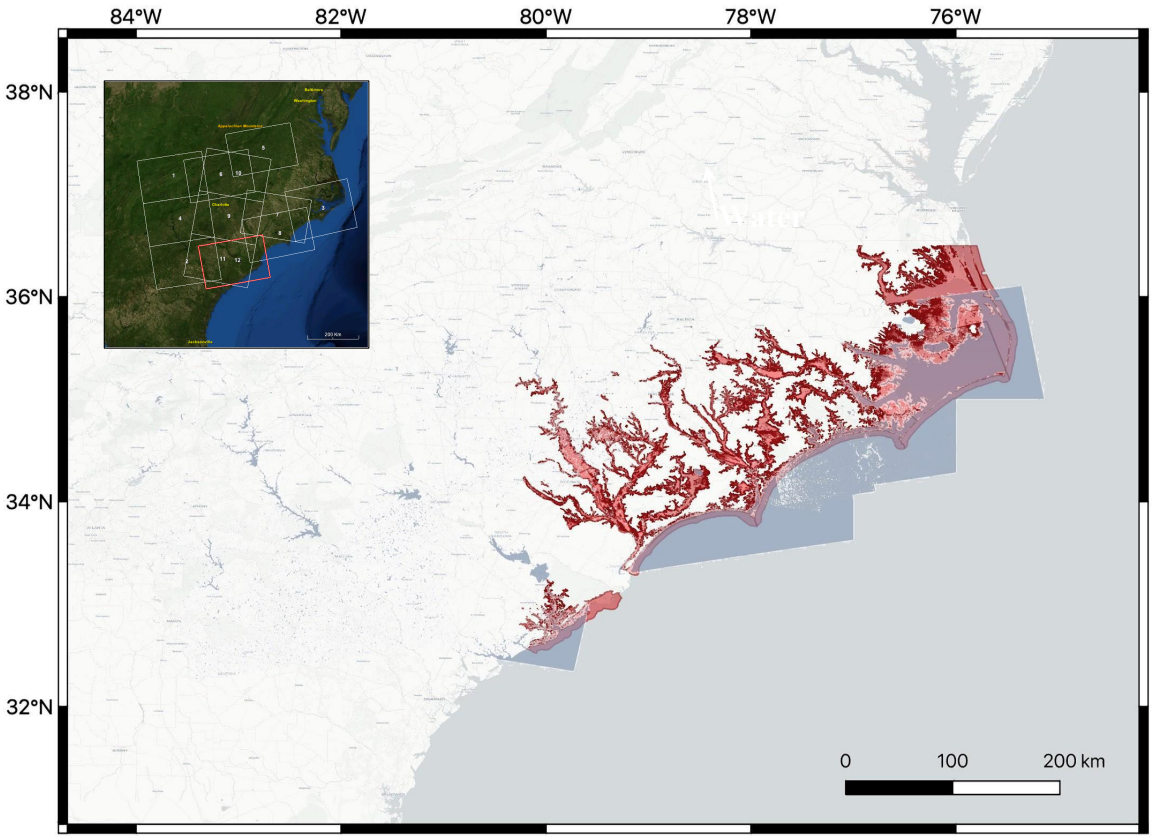

Figure 1 Map of inundated areas estimated by FEMA (red) and by the Sentinel-1 radar images (blue). The inset in the top left corner shows the footprint of the several radar images to create the composite water extent map. Acquisition times and other details concerning the radar images are available in Supplementary material.

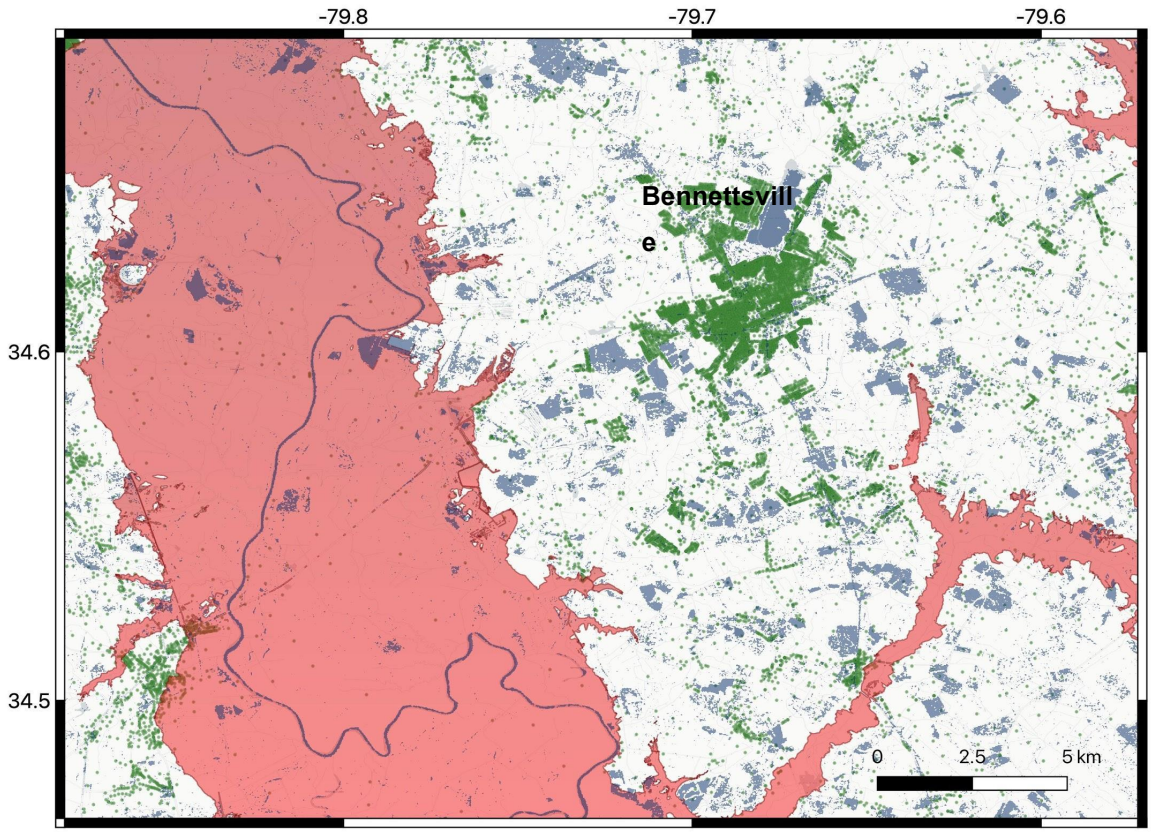

Figure 2 Map of inundated areas estimated by FEMA (red) and by Sentinel-1 (blue) near the town of Bennettsville, SC (34.6174° N, 79.6848° W). Green dots represent the locations of properties for this area.

5

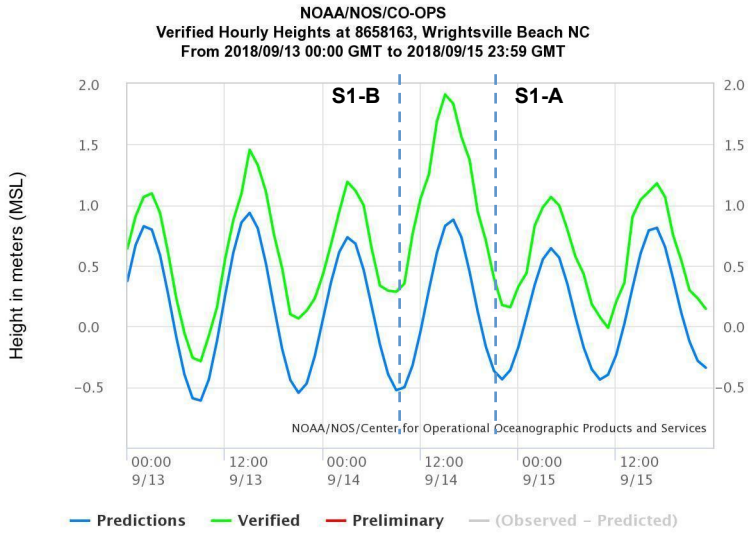

(a)

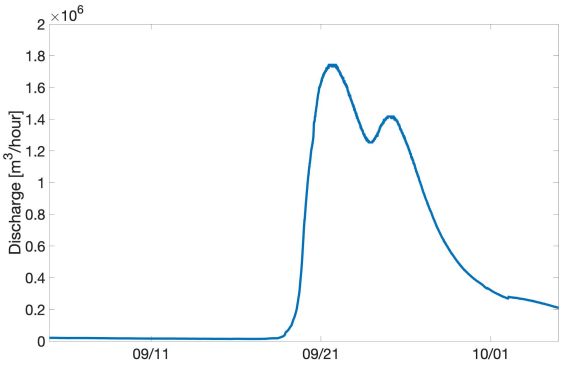

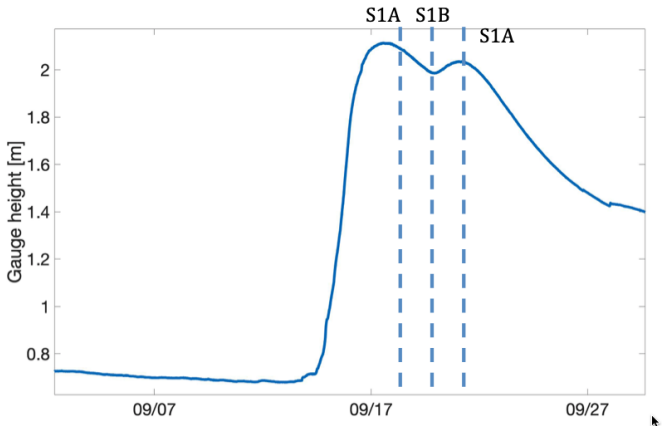

(b) (c)

Figure 3 Time series of a) tide gage mean sea level height (meters) recorded at Wrightsville Beach, NC and b) daily discharge (cubic feet per second) and c) daily gage height (feet) recorded at Lumber river (USGS gauge 02134170), NC between 1 September and 30 September 2018. In a) blue line refers to predictions where green squares to verified values. In a) data and plot was obtained from https://tidesandcurrents.noaa.gov/. For data plotted in b) and c) we obtained data and graphs from https://waterdata.usgs.gov/. In a) and c) we also report as dashed vertical lines the acquisition times of the available Sentinel-1 data.

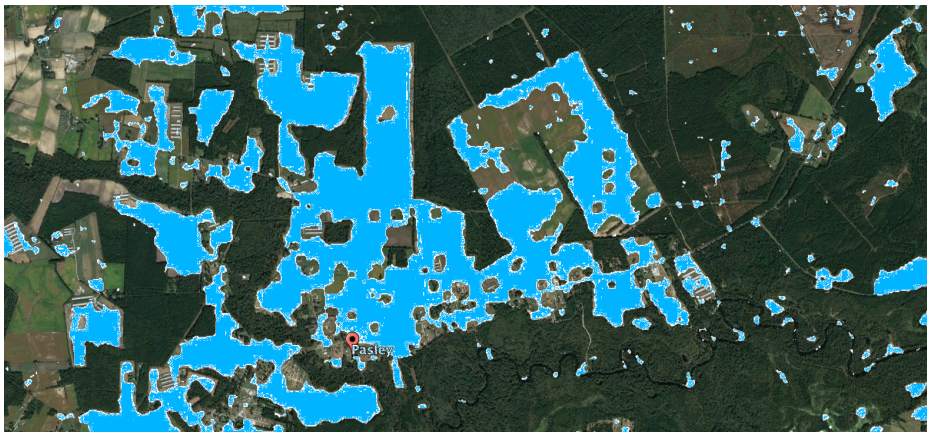

(a)

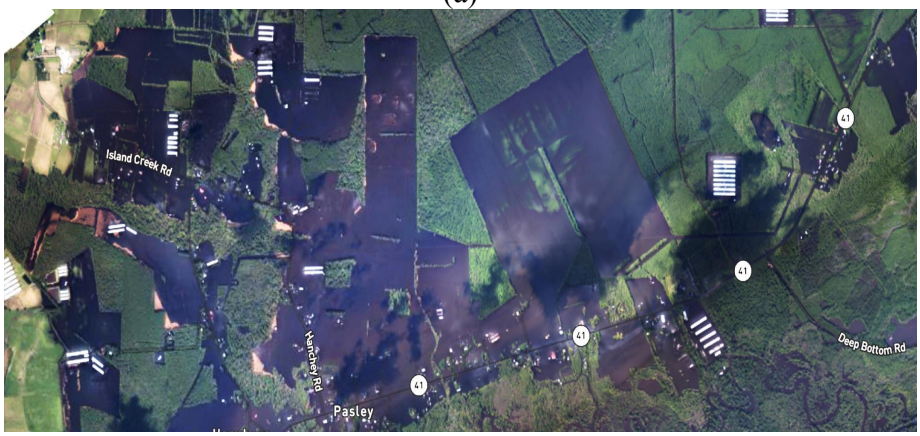

(b)

Figure 4 Flooded areas detected by a) Sentinel-1 data (light blue filled regions) on 19 September, 2018 nearby Pasley, Duplin County, NC (34.7854° N, 77.9005° W) and b) photograph of the same area collected on 18 September, 2018 by NOAA (https://storms.ngs.noaa.gov/storms/florence/index.html#7/35.360/-77.820). Here, dark blue regions show flooded areas.

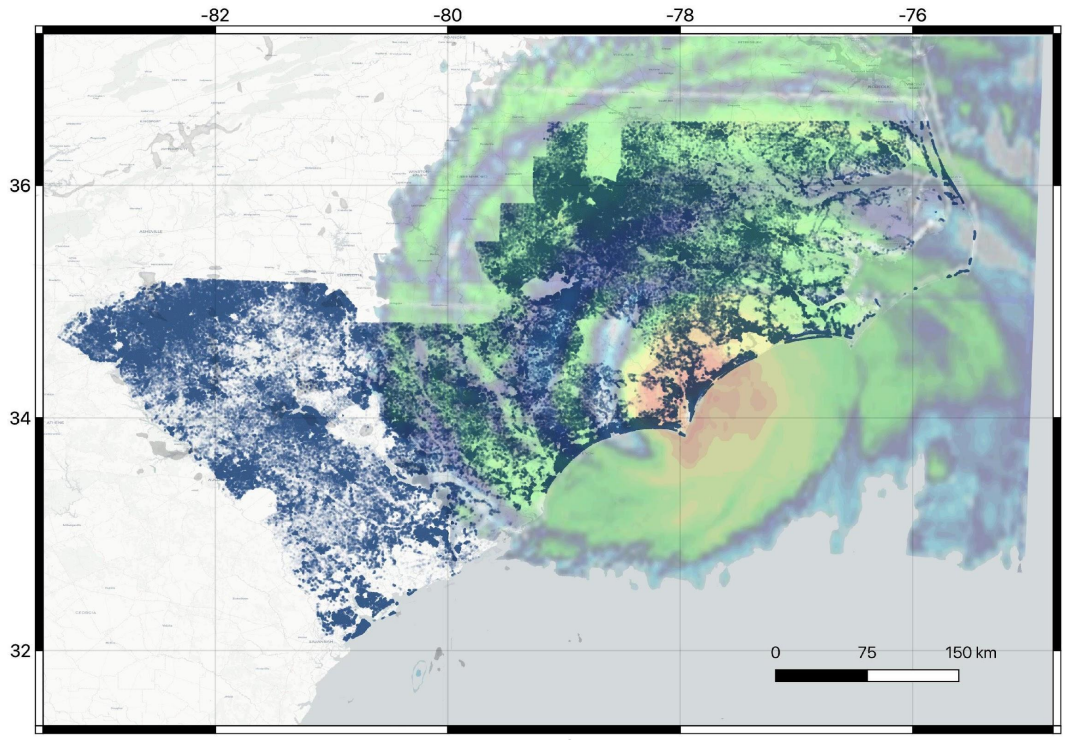

Figure 5 Distribution of properties within our database used to estimate the exposed property damage to Florence Hurricane. An image of the Hurricane Florence making landfall is also reported as a reference (Hurricane image courtesy: Cyclocane).

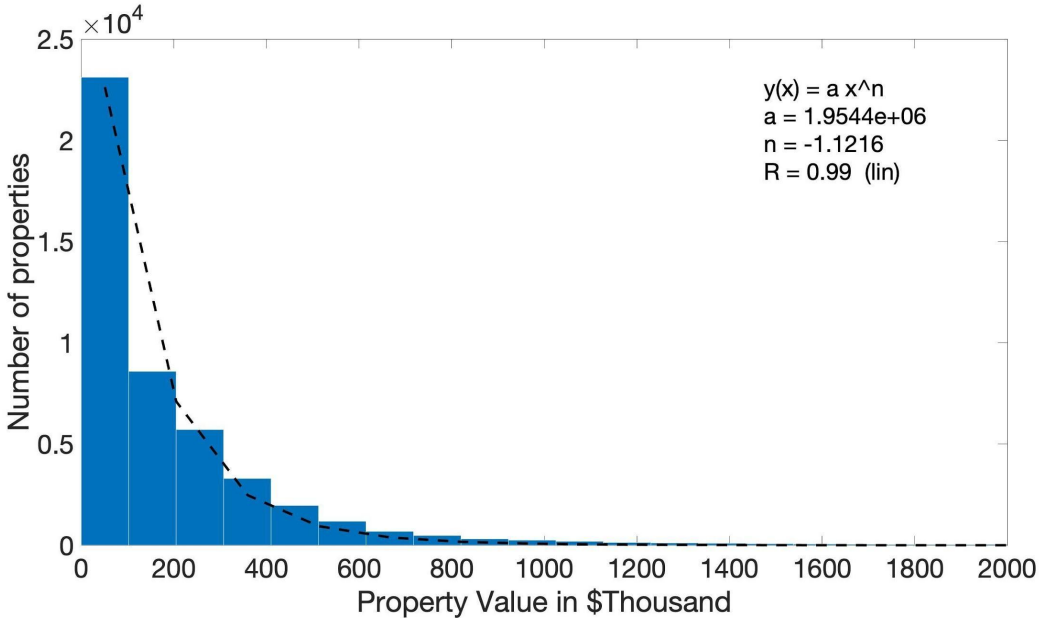

Figure 6 Distribution of the number of properties exposed to flooding as a function of property value. Dashed line represents the power law curve fitting the distribution. The parameters of the fitting power law function are reported in the top right section of the figure.

5

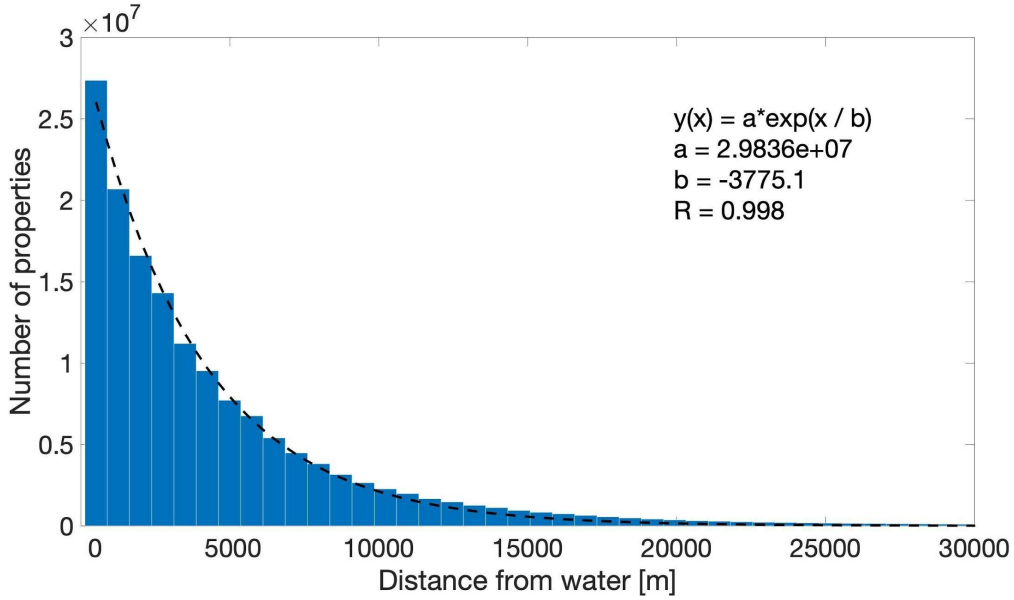

Figure 7 Number of properties as a function of distance from water bodies. Dashed line represents the power law curve fitting the distribution. The parameters of the fitting power law function are also reported in the top right section of the figure.

5

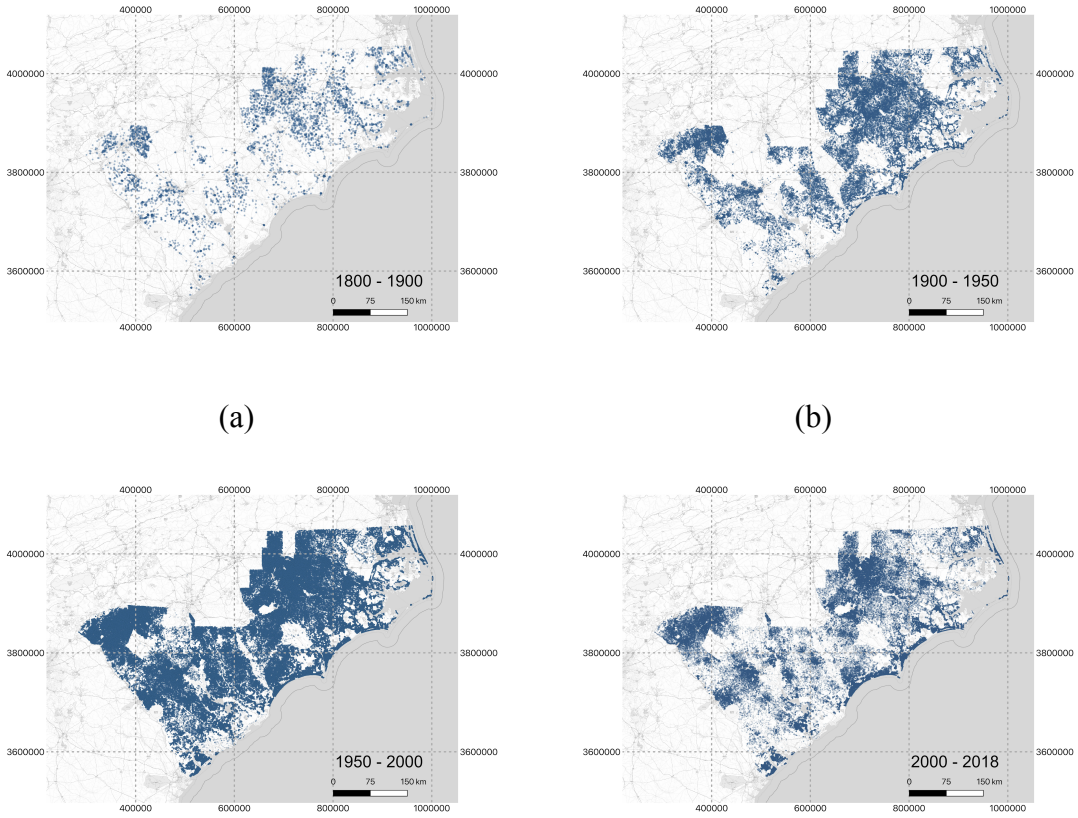

Figure 8 Spatial distribution of the properties within our database that were built during the a) 1800 – 1900, b) 1900 – 1950, c) 1950 – 2000 and d) 2000 – 2018 periods.

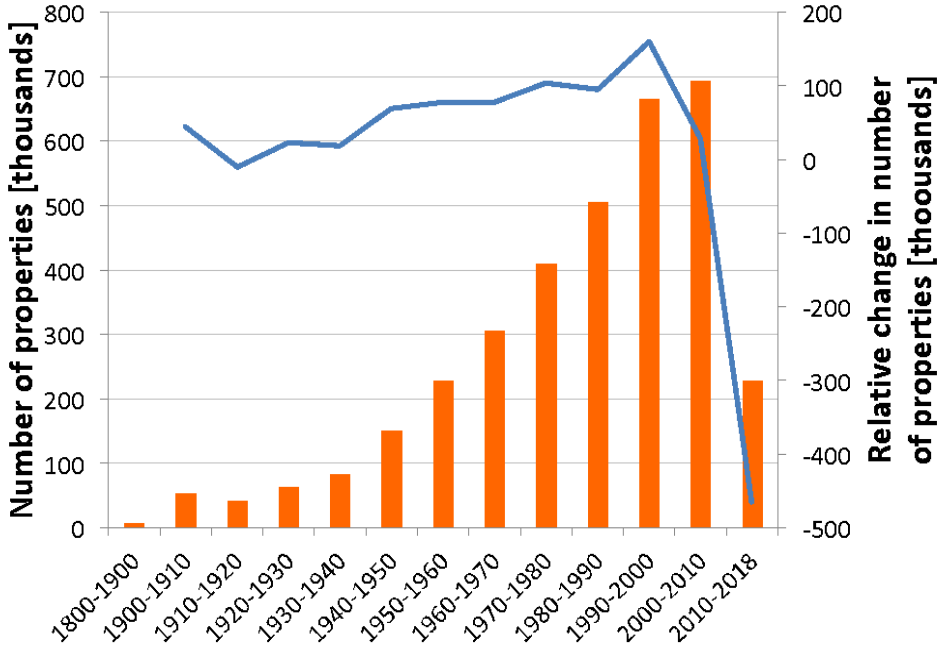

Figure 9 Number of properties (in thousands) built within our data record during different decades (red bars, left axis) and relative change between two consecutive periods (blue line, right axis). Note that the number of properties built between 1800 and 1900 are aggregated as a single value because of the small number of properties built during that period.

5

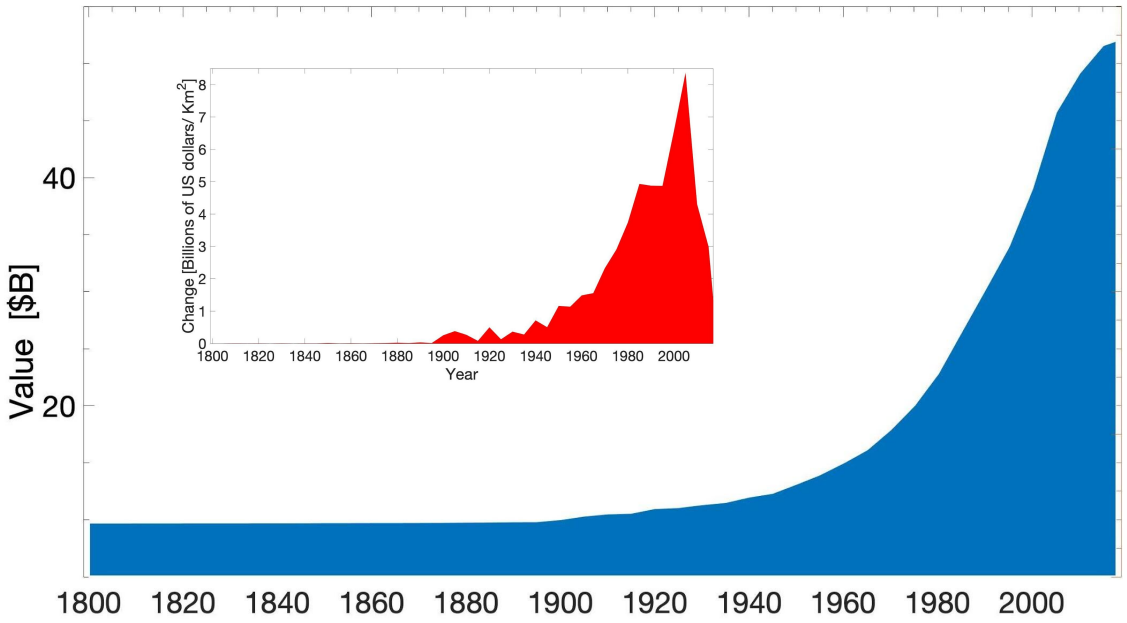

Figure 10 Time series of total value of exposed buildings (in 2018 USD) to the maximum flooded extent region between 1800 and 2018. The inset shows the relative change of the exposed area and value between two consecutive time steps (10 years).

5

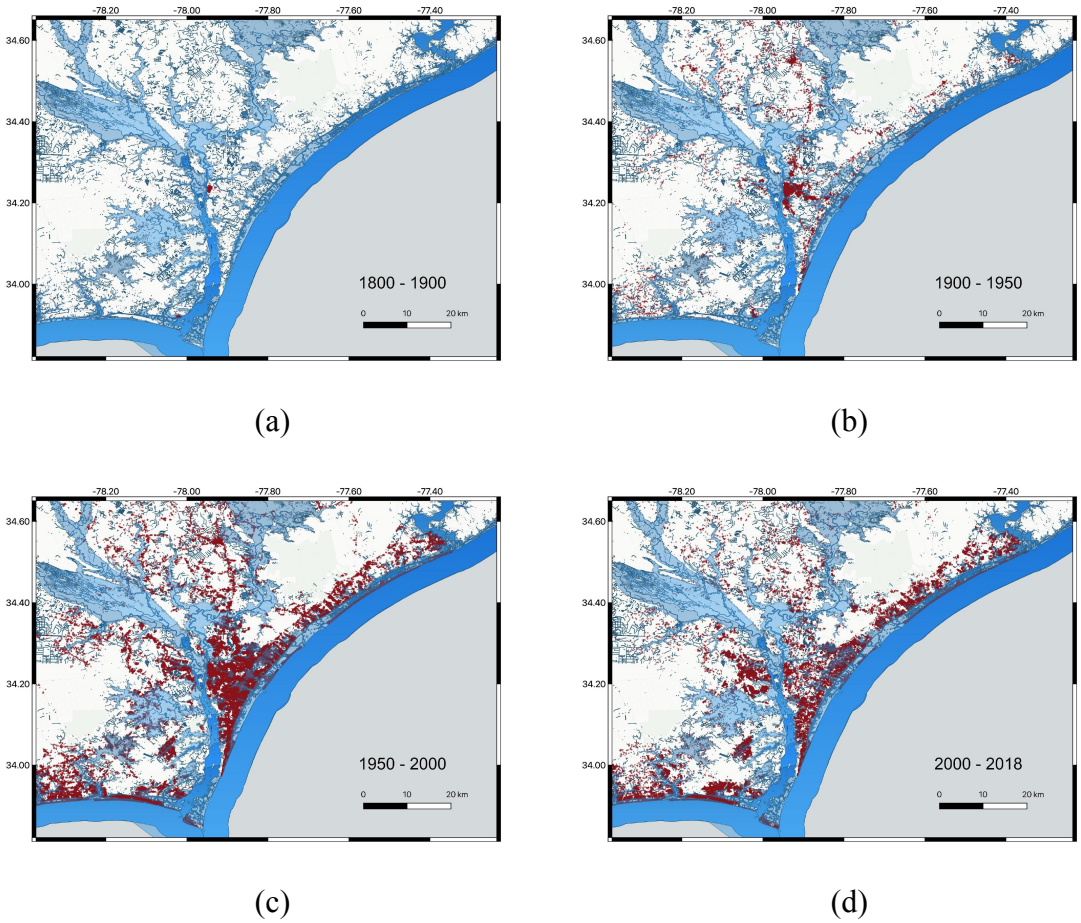

Figure 11 Distribution of properties (red dots) built a) before 1900, b) between 1900 and 1950, c) between 1950 and 200 and d) between 2000 and 2018 in proximity of Wrightsville Beach, NC where Hurricane Florence made landfall. Dark blue shows permanent body waters where light blue shows the flooded areas.

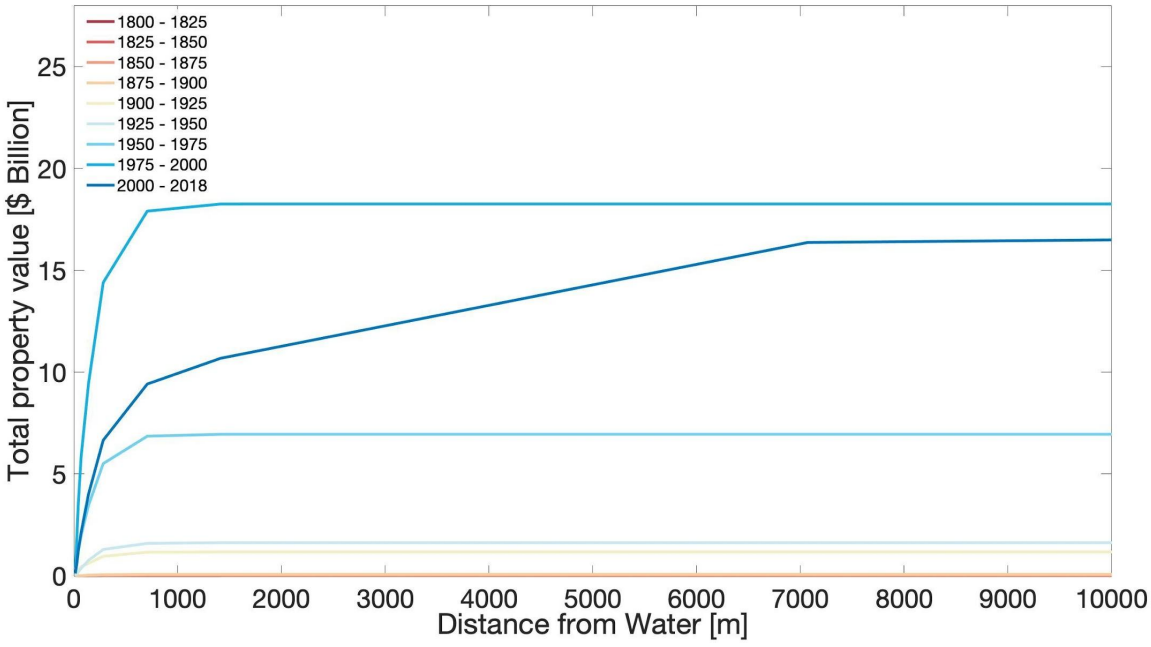

Figure 12 Total value within our database of properties exposed to flooding as a function of distance from water for the different periods reported in the inset.